CrossMark

Research Article

Quality by Design Approach for Developing Lipid-Based Nanoformulations of Gliclazide to Improve Oral Bioavailability and Anti-Diabetic Activity

Pravin Patel,[1] Sravanthi Reddy Pailla,[1] Nagarjun Rangaraj,[1] Hanumanth Srikanth Cheruvu,[1] Sujatha Dodoala,[2] and Sunitha Sampathi[1,3]

Abstract. The aim of the current investigation was to generate a self-nanoemulsifying drug delivery system (SNEDDS) of gliclazide (GCZ) to address the poor solubility and bioavailability. Ternary phase diagram was created with Capmul MCM C8 NF (oil), Cremophor RH 40 (surfactant), and Transcutol HP (co-surfactant) to distinguish the self-emulsifying region. A D-optimal design was employed with three variables, such as oil, surfactant, and co-surfactant, for further optimization of liquid (L)-SNEDDS. GCZ-loaded L-SNEDDs were analyzed for globule size, polydispersity index (PDI), and solubility. *In vitro* dissolution of optimized L-SNEDDS exhibited (F5) faster drug release (97.84%) within 30 min as compared to plain drug (15.99%). The optimized L-SNEDDS was converted to solid (S)-SNEDDS as a self-nanoemulsifying powder (SNEP) and pellets by extrusion-spheronization. Optimized S-SNEDDS were characterized using Fourier-transform infrared spectroscopy (FTIR), X-ray diffractometry (XRD), differential scanning calorimetry (DSC), and scanning electron microscopy (SEM). *In vitro* dissolution of SNEP (S3) and pellet were 90.54 and 73.76%, respectively, at 30 min. *In vivo* studies showed a twofold rise in bioavailability through SNEDDS with a significant decline in blood glucose levels compared to plain drug suspension suggesting a lipid-based system as an alternative approach for treating diabetes.

KEY WORDS: D-optimal design; extrusion spheronization; SNEDDS; pharmacokinetics; single-pass intestinal perfusion; self-nanoemulsifying powder.

INTRODUCTION

Gliclazide (GCZ), chemically known as [1-(3-azabicyclo (3,3,0)oct-3-yl)-3-(p-tolylsulfonyl) urea] (Fig. 1a) (1), belongs to second-generation hypoglycemic sulfonylureas, which is commonly used in the management of non-insulin-dependent diabetes mellitus (NIDDM)/type 2 diabetes. It has a capacity to slow down the advancement of diabetic retinopathy and also potent free radical scavenging activity *in vitro*. GCZ is very slightly soluble in water (0.19 mg/mL) with pKa of 5.8 exhibiting slow GI absorption rate with inter-individual variability (2). Poor dissolution and extensive first-pass

metabolism make the drug to have weary absorption rate, and hence, the oral delivery of the drug is challenging (3,4). The mean absolute bioavailability of the modified release tablets was reported as 97% (5).

To overcome the above limitations, many approaches were explored. Solid dispersion was reported for enhancing the oral bioavailability of GCZ; yet, there was only 1.5-fold increment (6). Moyano *et al.* investigated the beta-cyclodextrin inclusion complexes and found small improvement in the dissolution profile (7). Ranjith *et al.* prepared GLZ-loaded chitosan nanoparticles to sustain the drug release. The size of the nanoparticles was found to be around 900 nm, the drug entrapment was low, and the overall bioavailability enhancement is less (1.3-fold) (8). Also, Eudragit and PLCL nanoparticles were reported for sustained release of GCZ, where the pharmacokinetic study was not performed (9,10). However, all these formulations have achieved limited benefits in terms of solubility, drug loading, dissolution, or bioavailability. In this regard, lipid-based systems have evolved as alternative systems for efficient drug delivery due to their advantages; out of which self-nanoemulsifying drug delivery systems (SNEDDS) grabbed high attention for oral delivery of hydrophobic drugs, which practically enhances oral bioavailability (11). SNEDDS is a lipid-based formulation consisting of an

[1] Department of Pharmaceutics, National Institute of Pharmaceutical Education and Research (NIPER-HYD), Balanagar, Telangana 500037, India.
[2] Institute of Pharmaceutical Technology, Sri Padmavathi Mahila Visvavidyalayam, Tirupati, Andhra Pradesh 517502, India.
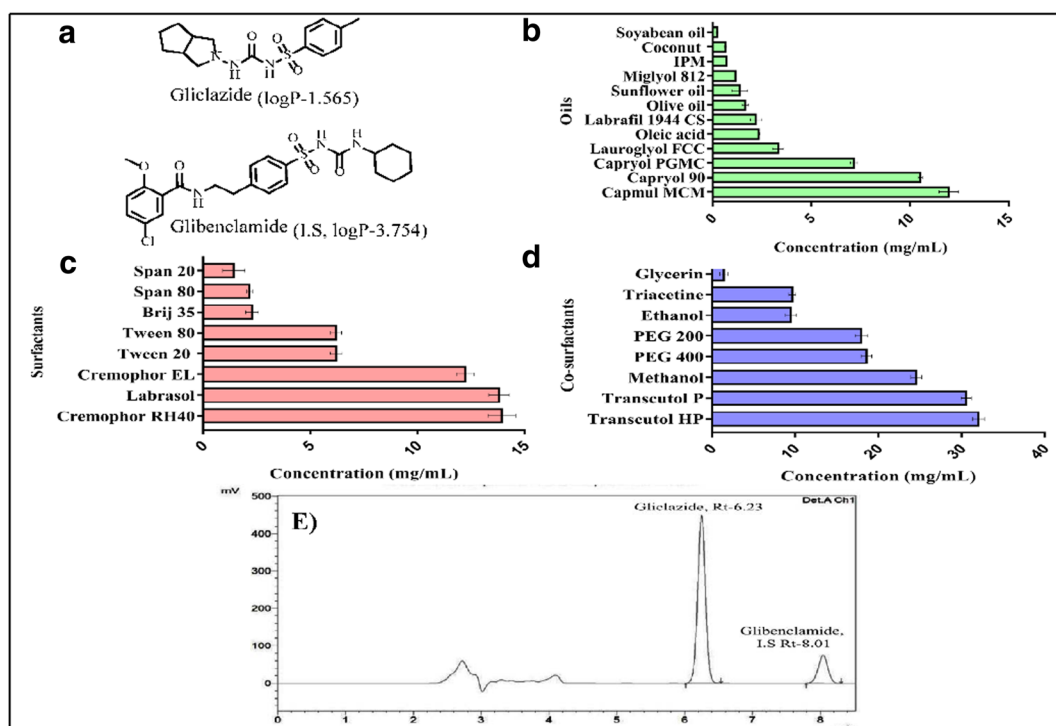[3] To whom correspondence should be addressed. (e–mail: sunithaniper10@gmail.com)

Fig. 1. a Chemical structure of gliclazide and glibenclamide (I.S.). **b–d** Solubility of gliclazide in different oils, surfactants, and co-surfactants, respectively. **e** Analytical chromatogram of gliclazide and glibenclamide (I.S)

isotropic fusion of oil, surfactant, and co-surfactant, which on exposure to aqueous medium lead to the evolution of an oil-in-water nanoemulsion instinctively (12). SNEDDS composed of a non-ionic surfactant, such as Cremophor RH 40, which is an o/w solubilizer and an emulsifying agent, facilitates trans-cellular and para-cellular absorption of the drug, and thus improves the bioavailability of poorly soluble drugs (13,14). SNEDDS are often composed in liquid state and placed into soft gelatin capsules. Yet, the soft gelatin capsules have few limitations like low drug compatibility, poor stability, drug leakage from gelatin shells, precipitation, capsule aging, scale up, and high production cost (15). Hence, it is beneficial to modify L-SNEDDS into solid dosage form referred to as solid (S)-SNEDDS (16), which can overcome above drawbacks with improved patient compliance. S-SNEDDS can be formulated as free-flowing powder, granules, and tablets, which are advantageous to obtain high stability.

Though GCZ-loaded L-SNEDDS was reported earlier, the authors focused only on characterization and *in vitro* evaluation (17). They have not studied the advantages of GCZ-loaded L-SNEDDS and S-SNEDDS in terms of bioavailability and anti-diabetic efficacy. Keeping this in view, L-SNEDDS was converted into self-nanoemulsifying powder (SNEP) and pellets *via* extrusion-spheronization technique *via* adsorption of GCZ L-SNEDDS onto various porous adsorbents.

To achieve this goal, GCZ-loaded L-SNEDDS was formulated using Capmul MCM C8 NF (oil), Cremophor RH 40 (surfactant), and Transcutol HP (co-surfactant) applying statistical design of experiments (DoE). DoE is a novel approach used to investigate, optimize the formulation, and process parameters by cost-effective screening in minimum time. Formulated L-SNEDDSs were analyzed for globule size, PDI, solubility, % transmittance, zeta potential, and drug release. Optimized L-SNEDDS was converted to S-SNEDDS using inert carriers, such as Aerosil, Sylysia, and Neusilin US2. The potential of L-SNEDDS and S-SNEDDS to raise the bioavailability of GCZ was evaluated along with its anti-diabetic efficacy in comparison to plain drug.

MATERIALS AND METHODS

Materials

GCZ was gifted by BAL Pharma Limited, Bangalore, India. Capmul MCM C8 NF was provided by Abitec Corporation (Janesville, Wisconsin). Capryol 90, Capryol PGMC, Labrasol, Lauroglycol FCC, Labrafil M 1944 CS, Transcutol P, and Transcutol HP were gifted by Gatteffose (FRANCE). Miglyol 812 was gifted by Leiutis Pharmaceuticals Pvt. Ltd. Hyderabad, India. Kolliphor® RH 40, isopropyl myristate (IPM), soybean oil, and olive oil were procured from Sigma-Aldrich®, India (Sigma® Chemical, St Louis, MO). Cremophor® RH 40 was gifted by BASF (Ludwigshafen, Germany). Sorbitan monolaurate 20 (Span 20), Sorbitan monooleate 80 (Span 80), and Triacetin were acquired from SD Fine Chem Ltd. India. Polysorbate 20 (Tween 20), Polysorbate 80 (Tween 80), PEG 200, PEG 400, and Brij 35 were acquired from Loba Chemicals Pvt. Ltd., Mumbai, India. Propylene glycol and glycerin were purchased from Final Chemical Limited Ahmedabad, India. Sylysia 350 and 770 fcp and Neusilin US2 were gifted by Fuji Sylysia Chemicals Ltd., USA. Croscarmellose sodium (Ac-di-sol), sodium carboxymethylcellulose (CMC), microcrystalline cellulose pH 101, and hydroxypropyl methylcellulose (HPMC) E5 were purchased from Accent Microcell Pvt. Ltd. Gujarat, INDIA. Methanol, acetonitrile, ethyl acetate, and all other chemicals were of analytical grade.

Methods

Solubility

The solubility of GCZ was estimated in different vehicles by means of shake flask method (18). In brief, surplus amount of GCZ was in corporate in 1 mL of every vehicle like oil (Capmul MCM C8 NF, Capryol 90, Capryol PGMC, Lauroglyol FCC, Oleic acid, Labrafil 1944 CS, Olive oil, Sunflower oil, Miglyol 812, IPM, coconut oil, soybean oil), surfactant (Cremophor RH 40, Labrasol, Cremophor EL, Tween 20, Tween 80, Brij 35, Span 80, Span 20), and co-surfactant (Transcutol HP, Transcutol P, PEG 400, PEG 200, ethanol, triacetin, glycerin). These samples were vortexed for 15 min to ensure proper mixing and subjected to continuous mixing at 37°C up to 72 h in a shaker water bath and centrifuged at 5000 rpm for 15 min. The samples were filtered through a Millipore membrane filter (0.45 μm). The supernatant was suitably diluted with methanol, and the soluble drug was estimated using HPLC (19).

HPLC Analysis

Equipment. Chromatographic separation was carried-out by an Inert sustain C_{18} column (150 × 4.6-mm diameter, 5-μm particle size) connected to a Shimadzu (Shimadzu, Cort, Japan) HPLC provided with a SAP-20A UV/visible indicator and LC-20 AD solvent pump unit. Mobile phase composed of acetonitrile and 0.1% formic acid (60:40, isocratic mode) was employed at a flow rate of 1 mL/min. Samples of 20 μL were injected, and eluents were monitored at a wavelength of 228 nm.

Preparation of Standards. GCZ and glibenclamide (internal standard) were accurately weighed, and the primary stock of 1 mg/mL was prepared. From this, a secondary stock of 100 μg/mL was prepared. Calibration standards were prepared in the range of 0.250–64 μg/mL.

Sample Extraction for Bioanalysis. Protein precipitation method was adopted to extract GCZ from plasma samples. Briefly, 250 μL of acetonitrile was added to 50 μL rat plasma and vortex mixed for proper extraction. Samples were centrifuged at 8500 rpm for 10 min, and the supernatant was analyzed by HPLC at a wavelength of 228 nm (20).

Method Validation. The developed method was validated for parameters, such as the limit of detection (LOD), limit of quantification (LOQ), linearity, accuracy, precision, specificity, recovery, and robustness (21).

Construction of Ternary Phase Diagram

From the solubility studies, the excipients (oil, surfactant, and co-surfactant) showing highest GCZ solubility were selected. A series of self-emulsifying systems (without drug) were prepared by varying the concentrations of selected vehicles. The oily phase was mixed with the S_{mix} (surfactant and co-surfactant mixture) and sonicated in a trembling water bath at 30°C for 5 min. To this

mixture, distilled water was added dropwise with mechanical shaking by a vortex mixer. Ternary phase diagram was built using Sigma Design version 12.0 software to identify the optimal self-emulsification region. The % transmission of blank SNEDDS was measured and the region, which showed clear or slight bluish dispersions of droplet size of ≤ 200 nm, was considered as the nanoemulsion region in the ternary phase diagram. The study was performed in triplicates (22).

Design of Experiments for the Preparation of GCZ L-SNEDDS

The D-optimal mixture design was used based on a three-component system: the oil X_1 (Capmul MCM C8 NF, % w/w), the surfactant X_2 (Cremophor RH 40%w/w), and co-surfactant X_3 (Transcutol HP % w/w). The range of each component was fixed based on the outcome of phase diagram. The droplet size (Y_1), solubility (Y_2), and polydispersity index (PDI) (Y_3) were used as responses (dependent variables) to know the effect of excipient concentration (23–25).

A total of 12 runs were generated by Design-Expert® software (version 11.0.2.0; Stat-Ease, Inc., Minneapolis, MN) to compose the L-SNEDDS. Linear, quadratic, special quadratic, and special cubic models consisting of three components are suitable models of mixture designs. Based on the evaluation of several arithmetical parameters, the best fitting mathematical model was chosen. The dependent and independent variables were mentioned with ranges in Table I.

The responses remained improved by a desirability function as per the method presented by Derringer and Suich (design-expert software). Response is connected with desirability function (d_i). The value "0" is assigned for unacceptable response and 0–1 for an acceptable response subjected to the nearness of the response to its goal value. The maximum desirability ($d_{i.max}$) function Eq. (1) is as follows:

$$d_{i.max} = Y_i - Y_{min} / Y_{max} - Y_{min} \tag{1}$$

Table I. Design of experiments (DoE) for the preparation of GCZ L-SNEDDS

RUN	X_1	X_2	X_3	Y_1	Y_2	Y_3
1	56.66	33.33	10	55.75	21.9	0.281
2	36.66	26.66	36.66	169.8	25.36	0.383
3	50	40	10	64.96	21.2	0.289
4	30	40	30	182.3	25.36	0.494
5	30	20	50	110.4	29.9	0.362
6	36.6	46.66	16.66	180.9	23.46	0.16
7	56.66	20	23.33	62.38	23.1	0.237
8	43.33	46.66	10	154.5	21.73	0.417
9	43.33	33.33	23.33	66.4	21.75	0.409
10	50	20	30	136.2	23.1	0.237
11	30	60	10	201.4	21.37	0.448
12	70	20	10	52.21	22.2	0.189

Note: X_1—Capmul MCM C8 NF, X_2—Cremophor RH 40, and X_3—Transcutol-HP
All the excipients were taken as % w/w
Y_1—globule size, Y_2—solubility, and Y_3—PDI

where $d_{i.max}$ is taken as distinct desirability of the responses and Y_i is the experimental result.

If $Y_i \leq Y_{min}$, then $d_{i.max} = 0$ and if $Y_i \geq Y_{max}$, then $d_{i.max} = 1$.

If the response is to be reduced, the desirability function Eq. (2) is defined as:

$$d_{i.min} = Y_{max} - Y_i / Y_{max} - Y_{min} \qquad (2)$$

where if $Y_i \leq Y_{max}$, then $d_{i.min} = 1$ and $Y_i \geq Y_{max}$, then $d_{i.min} = 0$.

Overall desirable value (*D*) is calculated *via* integration of individual desirable values as geometric mean ascertains the maximum desirable value by a comprehensive grid search over the domain for all the responses. *Validation of Design.* Validation of the statistical model prediction in droplet size, solubility, and PDI was carried by taking design points from the software.

Preparation of Gliclazide-Loaded L-SNEDDS

In brief, exactly weighed 30 mg of GCZ was dispersed in the mixtures of Cremophor RH 40 and Transcutol HP (S_{mix}), and the dispersions were gently wobbled at 30°C for 5 min. Capmul MCM C8 NF was added to the S_{mix} and sonicated for 15 min to get a clear dispersion. The resulting L-SNEDDS was preserved in air-tight containers at room temperature for further studies.

Characterization of L-SNEDDS

Self-Emulsification Time. Self-emulsification test was performed on all miscible self-nanoemulsifying system combinations according to the method suggested by Craig (22). Accurately, 0.6 mL of each self-nanoemulsifying system was placed in 200 mL of distilled water and agitated using magnetic stirrer at 100 rpm. The clarity of dispersion, spontaneity of emulsification, and apparent stability were observed.

Robustness to Dilution. L-SNEDDS was subjected to increasing dilutions (50, 100, and 1000 folds) using distilled water, simulated gastric fluid (0.1-N HCl, pH 1.2), and simulated intestinal fluid (phosphate buffer, pH 7.4) as media. After dilution, it is stored for 24 h to assess the stability and see if any physical change, such as phase separation and precipitation taking place. L-SNEDDS after suitable dilution with purified water (1:100) was subjected to centrifugal force (26). Droplet size was measured to check the influence of dilution on emulsion stability (27,28).

Determination of Globule Size, Polydispersity Index, and Zeta Potential. Mean globule size, PDI, and zeta potential were computed in triplicates at a light scattering angle of 90° by Malvern Nanosizer/Zetasizer® Nano-ZS ZEN 3600 (Malvern Instruments; UK) at 25°C (27). Each sample was suitably diluted to 50, 100, and 1000 folds with different media for comparison.

In Situ Single-Pass Intestinal Perfusion (SPIP) Method. To know the intestinal perfusion of L-SNEDDS, SPIP study was carried out following the previously reported methods (29,30).

In brief, the rats were segregated into two groups (pure drug and formulation) comprised of three animals each. The rats were anesthetized with thiopental sodium (50 mg/kg, intraperitoneal). The abdomen section of rat was cut up to 3–4 cm, and ileum segment of 10 cm was identified with ileo-cecal junction as a distal marker. The ileum and lumen were cleaned with saline by making semi-circular incisions at the two ends. Polyethylene tubing was inserted at the two ends and tied with a thread. The intestine was primarily infused with blank perfusion buffer (phosphate buffer saline) at a flow rate of 1 mL/min for 5 min using syringe pump (Olives India). Subsequently, the intestine was perfused with pure drug (in 0.5% *w/v* of CMC) and optimized L-SNEDDS (10 mM) at a continuous flow rate of 0.2 mL/min for a duration of 120 min, and perfusate was recovered for every 10 min. Isotonic saline-wet gauze was spread over the ileum segment. The length of the ileum segment was measured at the end of the perfusion. Perfusion samples collected at pre-fixed time points were evaluated by HPLC to estimate the concentration of drug. An outlet perfusate steady-state concentration achieved at different time points was considered for final calculations. The steady-state intestinal effective permeability (P_{eff}) was determined according to a parallel tube model.

$$P_{eff}, rat = -Q \cdot ln(C_{out}/C_{in})/60 \cdot 2\pi rl$$

where Q is the perfusion rate, r is the radius of the intestinal segment, l is the intestinal segment length, and C_{in} and C_{out} are the inlet and fluid transport corrected outlet solute concentrations, respectively.

Preparation of S-SNEDDS

S-SNEDDS was prepared from the optimized L-SNEDDS by two methods, *i.e.*, SNEP and pellets by extrusion-spheronization technique. *Self-Nanoemulsifying Powder.* The L-SNEDDS with less globule size, low PDI, and possessing good solubility was converted into SNEP by adsorbing onto the different solid porous carriers (inert), such as Neusilin US2, Aerosil 200, Sylysia 350, and Sylysia 770. In brief, 1 g of optimized L-SNEDDS was taken in a clean, dry glass mortar, and chosen solid inert carrier was gradually mixed in increment quantities and mixed to get a homogeneous free flowing powder. The prepared SNEPs were kept in a desiccator for further characterization and evaluation (31,32).

Preparation of Pellets by the Extrusion-Spheronization Technique. An optimized L-SNEDDS was converted into a solid pellet by extrusion-spheronization technique. In brief, Sylysia 350, MCC PH 101, HPMC E5, and ac-di-sol were mixed with optimized L-SNEDDS in a dry glass mortar to get a non-sticky solid powder (15). Few drops of distilled water were added for the formation of wet mass suitable for extrusion. The wet mass was extruded through 1-mm screen at 50 rpm for 5–8 min for the formation of extrudates. The

extrudates were then spheronized using a spheronizer (M.B.S 1029, 250406, Caleva, England) fitted with a screw of dimension 1 mm × 1 mm × 1 mm at 1000 rpm subjected to 8–12 min for the formation of spheres. The pellets were dried at 45°C (hot air oven) for 1 h and kept in a desiccator until further evaluation (33,34).

Determination of Liquid Adsorption Capacity, Micromeritics, and Reconstitution Properties

The fluid adsorption capacity of various carriers (Neusilin US2, Aerosil 200, Sylysia 350 and Sylysia 770) used in formulating SNEP was assessed by computing the quantity of inert porous carrier needed to adsorb 1 g of L-SNEDDS. Angle of repose, Hausner's ratio, Carr's compressibility index, bulk density, and tapped density were measured for SNEP (35).

For reconstitution property, the SNEP and pellets were dissolved in 100 mL of distilled water with gentle agitation on a magnetic stirrer at 100 rpm for 30 min. Further samples were filtered and analyzed for globule size, PDI, and zeta potential.

In Vitro Drug Release Studies

The dissolution was performed to compare the release pattern of a plain drug, L-SNEDDS, SNEP, and pellet in phosphate buffer (900 mL; pH 7.4) at a speed of 100 rpm and 37 ± 0.5°C using USP Type-II apparatus (DS 8000, LAB INDIA, Mumbai, India). Plain drug and formulations (equivalent to 30-mg GCZ) were placed in USP-II dissolution apparatus. At fixed time intervals, aliquots of 5 mL were collected and replaced with the phosphate buffer to maintain sink conditions. All the samples were clarified (0.45 μm) and analyzed by HPLC (20).

Characterization and Evaluation

Fourier-Transform Infrared Spectroscopy. The infrared spectrum of the plain GCZ, L-SNEDDS, Sylysia 350, SNEP, MCC PH 101, HPMC E5, Ac-di-sol (excipients), and the pellet was recorded on Fourier-transform infrared spectrophotometer (Shimadzu, Japan) in the range of 4000–400 cm^{-1} to find out interactions among the excipients used in the formulations.

Differential Scanning Calorimetry (DSC). DSC of plain drug, physical mixture of GCZ & Sylysia 350, optimized SNEP, and pellet was carried out using a differential scanning calorimeter (DSC Shimadzu, DSC-60, Kyoto, Japan). Accurately weighed samples were placed in a flat-bottomed standard aluminum pan and scanned at a heating rate of 20°C per minute in the range of 0–200°C under an inert nitrogen atmosphere at a flow rate of 40 mL/min.

X-ray Diffractometry. X-ray diffraction studies (XRD-7000 Shimadzu) of plain GCZ, optimized SNEP, and pellet were performed to investigate the change in crystallinity of the drug

when L-SNEDD transformed to S-SNEDD. The analysis was performed using copper (Cu Kα) radiation and graphite monochromatic voltage of 40 kV. The samples were scanned from 2 to 80°, at 2θ at a step size of 0.045° at the time of 0.5 s.

Scanning Electron Microscopy (SEM). Scanning electron micrographs for the plain drug, Sylysia 350, SNEP (S3), and pellet were taken using scanning electron microscope (Shimadzu, S-3700N, Japan) to study surface topography and shape. An accelerating voltage of 15 kV was used to capture SEM micrographs.

Pharmacokinetics. The experimental protocol was authorized by the Institutional Animal Ethics Committee (IAEC), NIPER-Hyderabad, Telangana, India (under protocol no. NIP/2/2015/PE/131). Male Wistar rats (180-200 g) were used for studying *in vivo* bioavailability of GCZ (plain drug suspension, optimized L-SNEDDS, SNEP (S3), and pellet). Animals were habituated to the laboratory conditions with temperature of 20 ± 2°C and 50–60% RH under light/dark climate for a week prior to experiments with complete access to food and water. Preceding the experiment, all the animals were fasted overnight with unrestricted access to water. All the rats were randomly segregated into four groups with six animals in each group. Plain drug (dispersed in 0.5% *w/v* CMC), L-SNEDDS, SNEP, and the pellet were orally administered (GCZ eq. to 6-mg/kg body weight). Retro-orbital plexus was used draw blood sample of 250 μL into EDTA coated tubes under mild anesthesia at pre-fixed time intervals (0, 0.25, 0.5, 1.0, 1.50, 2.0, 2.50, 3.0, 4.0, 5.0, 7.0, and 8.0 h). Blood samples were centrifuged at 7000 rpm up to 10 min using an Eppendorf centrifuge. The separated plasma was processed and analyzed according to the process mentioned in HPLC analysis (36).

Pharmacokinetic Parameters. Pharmacokinetic parameters, such as maximum plasma concentration (C_{max}), time taken for its occurrence (T_{max}), and area under the curve (AUC) for each rat, were calculated using the Phoenix software Winnonlin version 6.3 (Pharsight, Certara Company, USA). All the data are expressed as mean ± standard deviation, and one-way ANOVA was applied using GraphPad Prism software (version 4.00; GraphPad Software, San Diego, CA). The results were considered significant if P value is less than 0.05.

Anti-Diabetic Activity

Hypoglycemic activity of prepared formulations was tested in overnight fasted normoglycemic rats, which were grouped into five ($n = 6$). The control group received only vehicle (1 mL of 0.5% *w/v* CMC; p.o.), and the rest of the groups received 1 mL of a plain drug suspension, L-SNEDDS, SNEP (S3), and pellets (25 mg/kg; p.o.). All the animals were given glucose overload (2 g/kg, p.o.) post-30 min of drug administration. Blood samples were withdrawn (tail vein) prior to drug dosing and at 30-min interval up to 12 h of glucose administration. The fasting blood glucose level was measured using glucose-oxidase-peroxidase

active strips (Accu-check, Roche Diagnostics, GmbH, Germany) (37).

RESULTS AND DISCUSSION

Solubility

Solubility study of GCZ was performed in various selected vehicles as shown in Fig. 1b–d. Among all the tested oils, GCZ showed high solubility in Capmul MCM C8 NF (11.96 ± 0.49 mg/mL) and Capryol 90 (10.52 ± 0.11 mg/mL). Similarly, Cremophor RH 40 (13.93 ± 0.65 mg/mL) and Labrasol (13.80 ± 0.48 mg/mL) among surfactants and Transcutol HP (32.03 ± 0.73 mg/mL) and Transcutol P (30.55 ± 0.61 mg/mL) among co-surfactants have shown comparatively highest solubility. The analysis was done using HPLC. To select a suitable combination of oil, surfactant, and co-surfactant, miscibility and % transmittance were tested (Supplementary Table 1). The % transmittance was high with Transcutol HP than Transcutol P even though they are miscible in combination. Labrasol gave a turbid solution of poor % transmittance (≤ 7.75). With Capryol 90, the % transmittance is still less and it has shown turbidity with other combinations. Therefore, Capmul MCM C8 NF, Cremophor RH 40, and Transcutol HP were selected as oil, surfactant, and co-surfactant, respectively, for formulating L-SNEDDS.

HPLC Method Validation

HPLC method was developed with previously mentioned parameters, and the chromatogram is shown in Fig. 1e.

Limit of Detection and Limit of Quantification

LOD and LOQ are the concentrations where the signal to noise ratio (S/N) is above 3.3 and 10, respectively. Here, the LOD and LOQ were found to be 0.0625 and 0.250 μg/mL, respectively.

Linearity

The linearity of the compound was established in the range of 0.250 to 64 μg/mL, and the regression coefficient (R^2) was 0.999.   *Accuracy and Precision.* Accuracy and precision were assessed to know the quality control of samples, and the results are given in Supplementary Table II.

Specificity. The chromatograms of the sample are compared with the blank to determine the specificity.

Recovery. The response acquired from the concentration of the analyte extracted from the biological matrix is compared to the response of the pure standard to obtain percentage recovery. This study was performed at three concentrations (low, medium, and high) and un-extracted standards representing 100% recovery (Supplementary Table III).

Construction of Ternary Phase Diagram

Ternary phase diagram was constructed (without GCZ) to identify the self-emulsifying region and optimize the concentration of oil, surfactant, and co-surfactant for preparing L-SNEDDS in the ternary phase. The green solid line region in Supplementary Fig. 1 represents the more effectual self-emulsifying region. L-SNEDDS form a fine o/w emulsion within the self-emulsifying region with gentle agitation. Cremophor RH 40 reduces the interfacial tension and also lowers the bending stress of the film, which leads to formation of stable emulsion (38). Moreover, Transcutol HP (HLB-4), which is a co-surfactant, behaves as an amphiphile and is anticipated to enhance the interfacial fluidity of external surface of emulsifier in the micelles as a consequence of the entrapment of the previous in Cremophor RH 40 (HLB 14), improving the emulsification process upon dilution (11,39).

Design of Experiments

From the ternary phase diagram, oil (30–70%), surfactant (20–60%), and co-surfactant (10–50%) ranges were selected for the D-optimal design. A total of 12 experiments were conducted, and the responses observed were summarized in Table I.

Globule Size (Y_1)

Response (Y_1) of nanoemulsion was ranging from 52.21 to 201.4 nm. The model suggested by the design was linear, which was found to be significant. The adequate precision value was 8.70, which are more than the required value indicative of adequate signal and the model can be used for further analysis. ANOVA was performed to analyze the effect of factor over the response (Y_1), and the P value obtained was 0.0085. As shown in Fig. 2a, three-dimensional response surface plots and contour plots were constructed to interpret the correlation between dependent and independent variables. This correlation can be further studied by the actual regression equation given by the design.

$$\text{Globule size } (Y_1) = --0.82231X_1 + 3.23953X_2 + 2.14753X_3$$

This equation displays an inverse relation between the particle size and the concentration of Capmul MCM (X_1), whereas a direct relation with the levels of Cremophor RH 40 (X_2) and Transcutol HP (X_3). Increase in X_1 concentration along with decrease in the levels of X_2 and X_3 resulted in decrease in particle size. This relation can be justified by reduction in the droplet size from 201.4 to 52.2 nm, when the amount of Capmul MCM C8 NF was increased from 20 to 70% keeping Cremophor RH 40 and Transcutol HP (X_3) at low levels of 20 and 10%, respectively.

Solubility (Y_2)

Solubility (Y_2) of the drug plays an important role in the formulation. Hence, it is selected as the response, and after the experimentation, the solubility ranged from 21.1 to 29.9 mg. Linear model was applied for the regression analysis, and it was found to be significant with adequate precision value 12.58, which is more than the required value indicative of adequate signal and the model can be used for further analysis. Further ANOVA was performed to analyze the effect of factors on the response (Y_2), and the P value
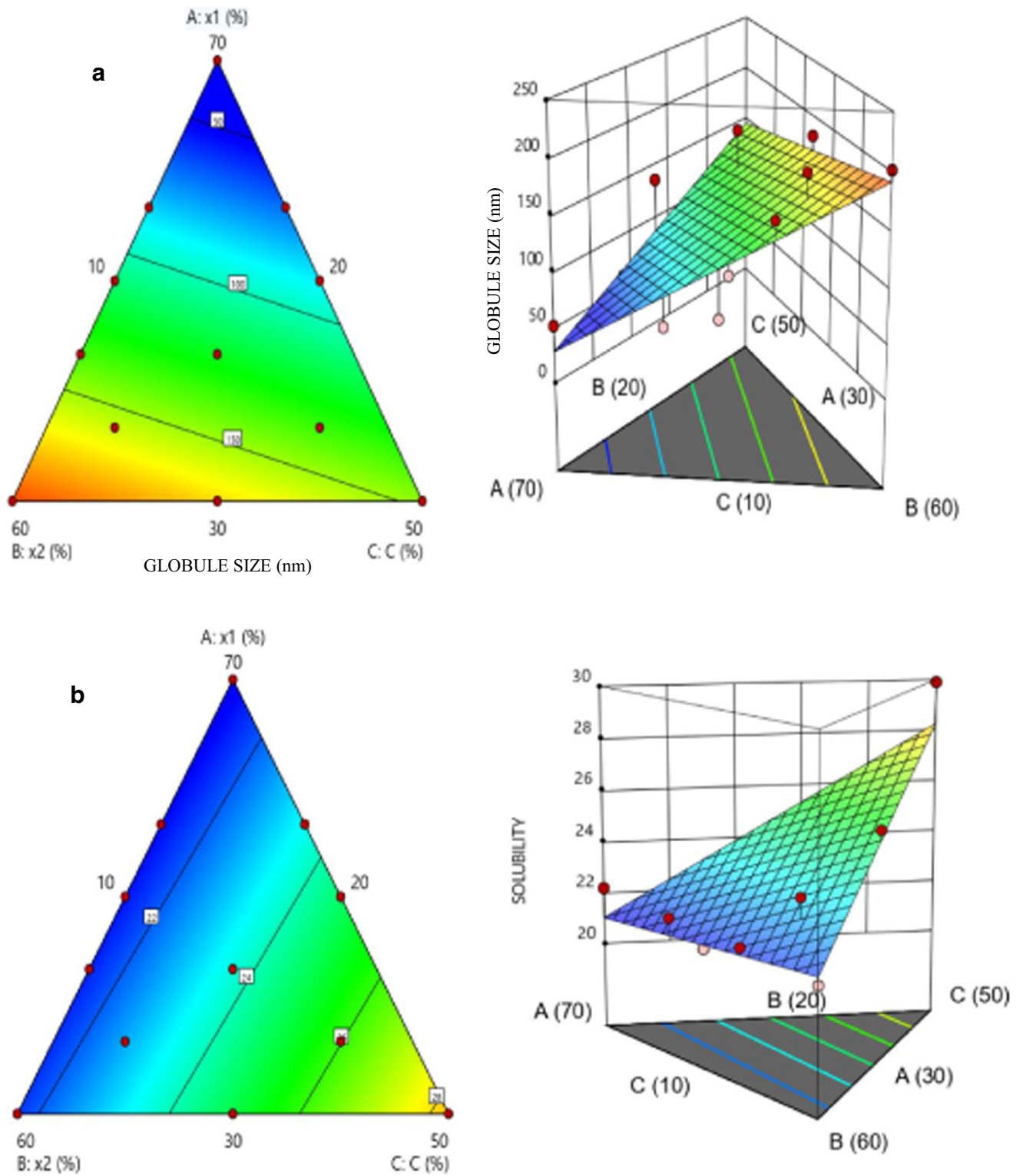
Fig. 2. a Response surface and contour plots showing the effects of variables on globule size (Y1). **b** Response surface and contour plots showing the effects of variables on solubility (Y2). **c** Response surface and contour plots showing the effects of variables on PDI (Y3). **d** Overlay plots obtained by criteria of low globule size, low PDI, and solubility greater than 25 mg/mL
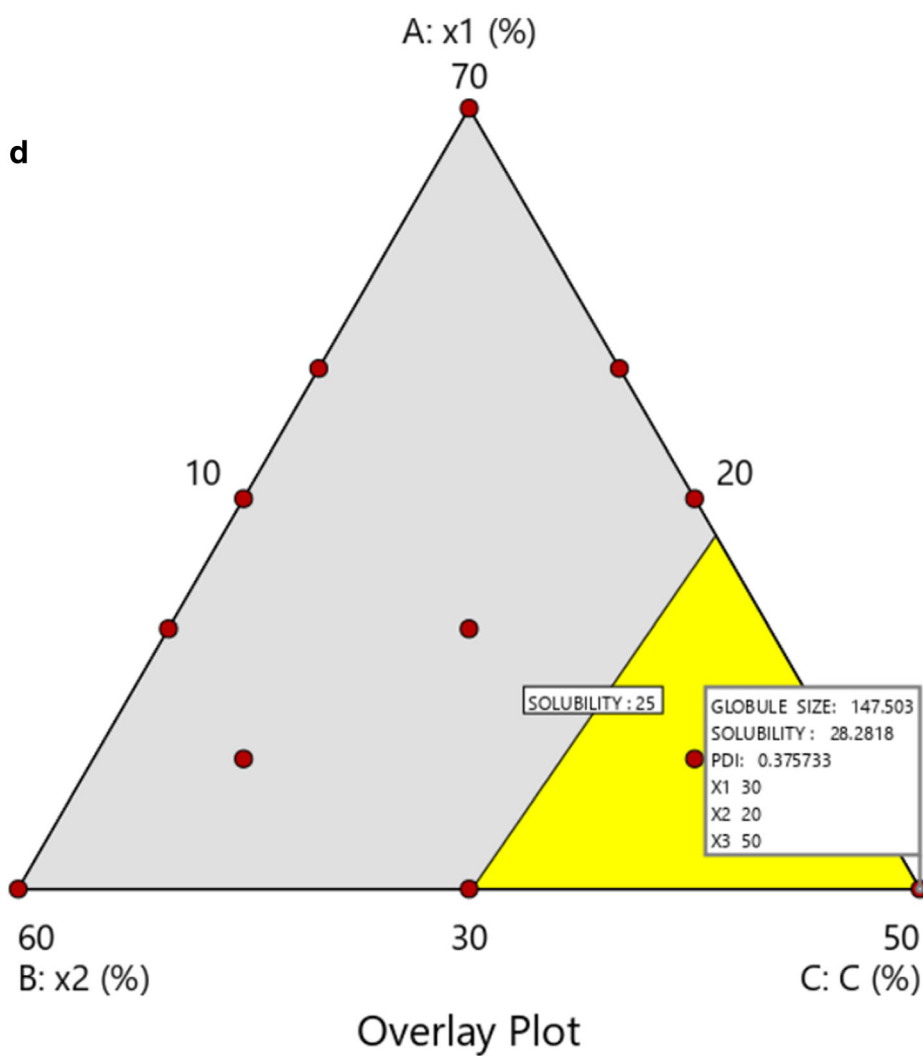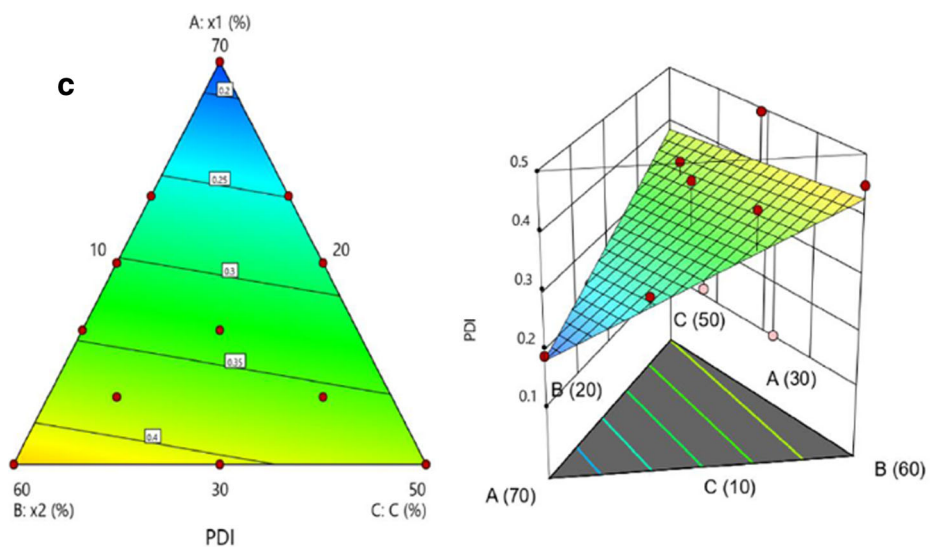
Fig. 2. (continued)

obtained was 0.0004. As shown in Fig. 2b, the contour, 3D surface plots, and the solubility are affected by all the factors. This correlation can be explained by the actual regression equation, which is

$$Solubility\ (Y_2) = 0.18898\ X_1 + 0.20500\ X_2 + 0.37025 X_3.$$

All the factors have positive impact on the response, whereas the response of X_3 has prominent impact, which can be noticed with the increase in solubility up to 29.9 mg when the levels of X_1, X_2, and X_3 are 30, 20, and 50, respectively.

Polydispersity Index (Y_3)

PDI gives the broadness of the prepared formulation, whether the prepared formulations are mono or heterodisperse. In these trials, the PDI values varied from 0.160 to 0.494. Reduced special quartic model was applied for the regression analysis, and it was found to be significant with adequate precision value 11.23, which is more than the required value indicative of adequate signal and model can be used for further analysis. Further ANOVA was performed to analyze the effect of factors on the response (Y_3), and the P value obtained was 0.0029. As shown in Fig. 2c, the contour, 3D surface plots, and the PDI are affected by all the factors. This correlation can be explained by the actual regression equation, which is

$$\begin{aligned} Polydispersity\ index\ (Y_3) = &\ 0.168X_1 + 0.486\ X_2 + 0.375X_3 \\ &+ 33.86\ X_1{}^2 X_2 X_3 - 29.32\ X_1 X_2{}^2 X_3. \end{aligned}$$

ANOVA, regression analysis, and factor co-efficient with corresponding P values of each response were provided in Supplementary Tables IVa, IVb, and IVc, respectively.

To obtain the desirability values, the criteria were set to minimize the response Y_1 and Y_3 and to maximize the response Y_2. The higher the desirability value, the higher is the assurance of obtaining the desired values with the provided formulations. Desirability value of 0.806 was obtained for the solution, which is the same as that of the formulation F5 ($X_1 = 30$ mg, $X_2 = 20$ mg, and $X_3 = 50$ mg). The overlay plot for the same was generated, and the region in yellow color represents the area of choice where the desired results shall be obtained and the gray area represents the out of scope area shown in Fig. 2d.

Validation of the design was done by confirmation trial. The result obtained by the run was compared with the values predicted by the design, and the difference between these values was calculated. The reliability of the design used was assured by the low value of biasness obtained.

Characterization of L-SNEDDS

Assessment of Self-Emulsification Time and Robustness to Dilution

Emulsification studies clearly distinguish the emulsification potential of several surfactants. A proper mixture of low and high HLB surfactants is imperative to develop a stable self-nanoemulsifying system. An adequate ratio with perfect blends of surfactants with HLB value of 14–16 and 4.2 for Cremophor RH 40 and Transcutol HP, respectively, aids in the highest emulsification efficiency (98.05%). The mixtures prepared using Labrasol as surfactant exhibited a low transmittance value ($< 10\%$), which is indicative of poor emulsification capacity. Though the selected surfactants in this study have a HLB value in the range of 14–16, the experimental variation in their emulsification capability may be ascribed to the variation in their arrangement and chain length (13). This combination of surfactant and co-surfactant resulted in lucid nanoemulsion with short time for emulsification (11).

Also, after 50, 100, and 1000 times dilution with water, pH 1.2 and pH 7.4, there was no precipitation, cloudiness, or separation even after 72 h. The resulting emulsions were satisfactory with less particle size (< 201 nm) demonstrating their toughness to dilution.

Globule Size, PDI, and Zeta Potential

Globule size, PDI, and zeta potential are critical parameters, which in turn affect the bioavailability of drug. Globule size limits the drug release and absorption, since smaller particles come up with a high surface area for faster drug diffusion. A perfect ratio of oil, surfactant, and co-surfactant contributes to stable and efficient SNEDDS that undergoes spontaneous emulsification because of its low globule size. A variation in the length of fatty acid carbon chain and degree of unsaturation of the selected oil and surfactant will greatly determine the stability of the formed emulsion (40). As shown in Fig. 3, globule size was calculated by zeta sizer, and the results were found to be in the range of 52.21 to 201.4 nm, which indicated nanometric size range. The globule size of the nanoemulsion is believed to be an important parameter that results in less emulsification time with improved absorption *via* lymphatic uptake and thereby causing a successive intensification in therapeutic effectiveness of the drug (41,42). Capmul MCM C8 NF is a good solvent for lipophilic drugs, and besides, it aids in self-dispersibility of formulation upon hydration. Further, it is likely that the use of high HLB surfactant possess an advantage in increasing interfacial fluidity and emulsification of SNEDDS upon dilution with water (39). Cremophor RH 40 (HLB 14), a non-ionic solubilizer, and Transcutol HP (HLB 4), being a co-solvent, are responsible for the formation of small globule size with low PDI in the presence of fatty acids (22). Among the prepared formulations, F5 was found to have a droplet size of 110.4 ± 1.9 nm and PDI of 0.262 with zeta potential -30.1 mV (Fig. 3). A higher value of zeta potential interprets an increase in electrostatic repulsive force, therefore, ruling out the probability of coalescence (43,44).

Preparation and Evaluation of Self Nanoemulsifying Powder and Pellets

S-SNEDDS concept was evolved to overcome the stability and compatibility issues that arise upon incorporation of L-SNEDDS into the capsule. The L-SNEDDS (F5) was changed into SNEP by adsorbing onto porous inert
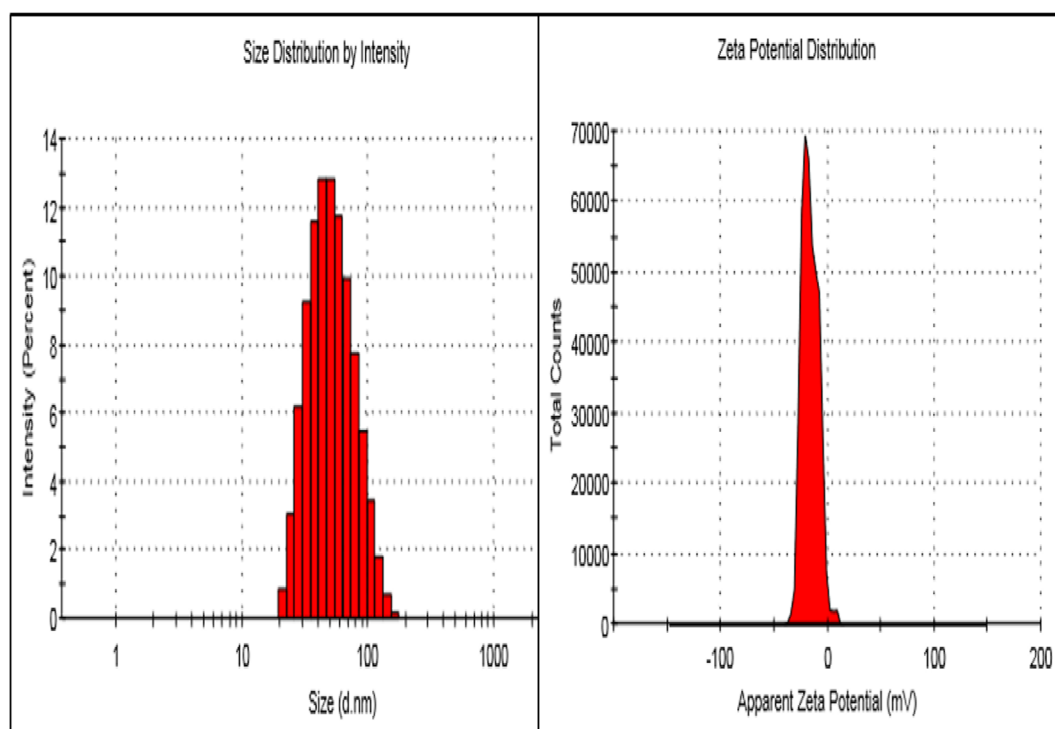
Fig. 3. Globule size and zeta potential results

carriers. The liquid adsorbing capacity and flow properties are given in Table II. Amid the various adsorbent carriers, Sylysia 350 has shown better flow properties with a minimum amount for adsorption (380 mg for 1 g of L-SNEDDS). The ratio of excipients to L-SNEDDS needs to be tailored in such a manner that there is effective adsorption without any loss of drug during the process. Sylysia 350 is an amorphous micronized silica characterized by high porosity with an average particle size of 3.9 μm and has a bed surface area of 300 m^2/g, frequently used to adsorb lipid formulations (45). Sylysia 350 is widely used as a powdering agent and carrier for liquid medicaments with good flowability, which helps in the conversion of powder to pellets and does not affect the quality and stability of drug on storage. SNEP prepared using Sylysia 350 is having a Carr's index value of 16.75 and Hausner's ratio of 1.25 and hence can be regarded to possess good flow properties. SNEP was converted to nanoemulsifying system and observed that on dilution, there was an increase in the particle size. However, it was below 200 nm (189.2 ± 14.2 nm), and a slight increase in particle size may be owed to the time taken for surfactant and co-surfactant to release from powder matrix. Further, the prepared SNEP was evaluated for *in vitro* dissolution and

chosen for extrusion spheronization to prepare pellets for easy handling, which can improve the patient compliance. The concept of combining the benefits of self-emulsifying system with pellets prepared by extrusion spheronization technique was established by Newton *et al.* (42). Based on the micromeritics and *in vitro* dissolution studies, SNEP formulation containing Sylysia 350 (S3) was chosen for further studies because of its high adsorbing capacity and less particle size with enormous surface area. The composition of optimized pellets prepared using SNEP (S3) was shown in Supplementary Table V. The physical state of the drug in SNEP and pellet formulation was further investigated as it influences release characteristics (46).

In Vitro Drug Dissolution Studies for L-SNEDDS, SNEPs, and Pellet

Cumulative percent drug release was carried out in phosphate buffer (pH 7.4) using a USP apparatus type II. The drug release profiles of plain drug and F5 (L-SNEDDS) are shown in Fig. 4a. Formulation F5 (97.84%) showed higher drug release within 30 min compared to plain drug dispersion (15.99%), which is significantly low ($P < 0.05$). Greater

Table II. Liquid adsorbing capacity and flow properties of various adsorbents for SNEP preparation from L-SNEDDS(F5)

Code	Solid carrier	Drug (mg)	Carrier required for 1-g L-SNEDDS(F5) (in mg)	Bulk density	Hausner's ratio	Tapped density	Carr's index	Angle of repose
S1	Aerosil 200	30	417 ± 24.50	40.9	1.23	50.21	19.05	26.21
S2	Neusilin US 2	30	732.5 ± 17.67	45.4	1.19	54.11	16.09	22.6
S3	Sylysia 350 FCP	30	380 ± 14.14	36.06	1.25	43.32	16.75	25.43
S4	Sylysia 770 FCP	30	1145.5 ± 26.89	55.79	1.21	67.75	17.65	24.84

availability of the dissolved GCZ and nanosized droplets of emulsion could have led to higher drug release, which is also supported by other authors (47). Hence, F5 was further selected for transformation of L-SNEDDS to S-SNEDDS, and dissolution was carried out for the same. Dissolution was performed for all the prepared SNEPs to know the effect of different carriers.

The comparative dissolution profiles of plain GCZ, S1 (Aerosil 200), S2 (Neusilin US2), S3 (Sylysia 350 FCP), and S4 (Sylysia 770 FCP) are shown in Fig. 4b. The results show that SNEP prepared with Sylysia 350 (95.13%) showed faster drug release within 30 min followed by S2 (91.84%). Less drug release was seen for both S1 and S4 (around 86%) when compared to the plain drug. Though there was an insignificant variation in drug release among S2 and S3 within 30 min, percent drug released within 5 min was greater for S3. The percent drug release from plain drug, S3 SNEP, and pellet was shown in Fig. 4c. The percent drug release within 30 min was 73.76 and 95.13% for pellet and SNEP, respectively. The average dispersing droplet size formed by S3 and pellets with Sylysia 350 was in the order of 152.45 and 189.2 14.22 nm, respectively. The faster dissolution kinetics of powder and pellet was in accord by smaller size of droplets produced, which render a great surface area for drug diffusion and rapid emulsification of L-SNEDDS also led to higher dissolution (22). Superior dissolution is also attributed to huge surface area of the Sylysia 350, and its high porous nature helps in uptake of release medium and simultaneously leading to rapid emulsification.

In Situ Single Pass Intestinal Perfusion Method

In spite of the good *in vitro* results, most of the drugs fail to show the *in vivo* activity due to the reasons like poor absorption, water insolubility, and physical instability. Intestinal mucosa forms the major barrier for controlling the process of absorption. Regarding the same, we conducted the SPIP study for determining formulation efficiency in an intact rat model. Intestinal permeability of plain drug and L-SNEDDS was assessed in rat ileum. Effective permeability (P_{eff}) was determined from the steady-state drug concentrations in the collected perfusate. Results showed that there was an improvement in effective permeability of drug from $0.08 \pm 0.002 \times 10^{-4}$ to $0.3 \pm 0.04 \times 10^{-4}$ cm/s. The main advantage of *in situ* SPIP technique is integral physiological conditions in experimental animals. This method helps in predicting intestinal absorption in humans as it relates to the local absorption rate across the epithelial barrier. Our results predicted that drug delivery in nanoemulsion increased the intestinal permeability due to reasons like reduced particle size, increased surface area, increased solubility, and better dissolution.

Characterization and Evaluation

Fourier Transform Infrared Spectroscopy for SNEP and SNEDDS Pellets

To reveal the compatibility among the components, IR spectra of plain GCZ, excipients, and formulations (L-SNEDDS, SNEP, and pellets) were recorded as shown in Fig. 5a, b. The plain GCZ showed distinctive absorption peaks at 3270, 2932, 1707, 1596, and 1349 cm^{-1}, whereas Sylysia 350 exhibited broad absorption peaks at 1080.29, 972.22, and 799.58 cm^{-1}. The unique peaks of the drug at 2925, 2857.37, 1737.54, 1456.93, and 1350.39 cm^{-1} were retained in L-SNEDDS, SNEP, and pellet formulation. However, in SNEP, the disappearance of remaining peaks of GCZ could be related to over lapping with Sylysia peaks, and no additional peaks were detected. Similarly, the SNEDDS pellet showed the absorption peaks of the drug as seen in plain drug revealing the absence of any chemical interaction among drug, porous carrier, and other components, thus confirming the compatibility of excipients.

Differential Scanning Calorimetry

DSC thermograms of GCZ, a physical blend of drug and Sylysia 350, SNEP (S3), and pellet, are shown in Fig. 6. Plain GCZ confirmed a pointed endothermic peak at 169.86°C corresponding to its melting point. In physical mixture, an endothermic peak of drug was seen at 163.24°C with less intensity, and the carrier exhibited a diffused peak at around 230.2°C. But, in case of SNEP (S3) and pellet formulations, a broad diffused peak was seen, which is an evidence of transforming crystalline state of drug to amorphous form or a reduced crystallinity of GCZ in optimized formulation (14,48) that may be further confirmed from powder XRD.

X-ray Diffraction

The XRD for the plain drug, SNEP (S3) and pellet are shown in Fig. 6b. The XRD prototype of GCZ shows spiky peaks at diffraction angles (2θ) of 11, 15, 17, 18, 21, and 22 showing crystallinity of drug. XRD spectra of SNEP and pellet revealed that there was no drug precipitation during conversion of L-SNEDDS to SNEP and pellets. Drug peaks were also noticeable in XRD pattern of pellets but with low-intensity characteristic peaks of GCZ and even the absence of some peaks indicating the transformation of GCZ from crystal-like to unstructured form in S-SNEDDS (49) and hence could be the reason for faster dissolution for SNEP and pellet.

Scanning Electron Microscopy

The external surface of the drug (plain), Sylysia 350, S3 SNEP, and pellets was observed through SEM, and the illustrations are shown in Fig. 7. Plain drug disclosed a combination of unevenly formed crystals of numerous dimensions, whereas Sylysia 350 powder was found to be as a very fine granular porous powder. SEM image of SNEP (S3) and pellet indicated the absence of any drug crystals on the pellet surface, which confirmed the solubilization state of a drug. The lack of the distinctive crystalline structure of GCZ in SNEP (S3) designates the conversion of the drug to unstructured or as molecular condition (50). Similarly, pellets were spherical in shape with a rough surface.
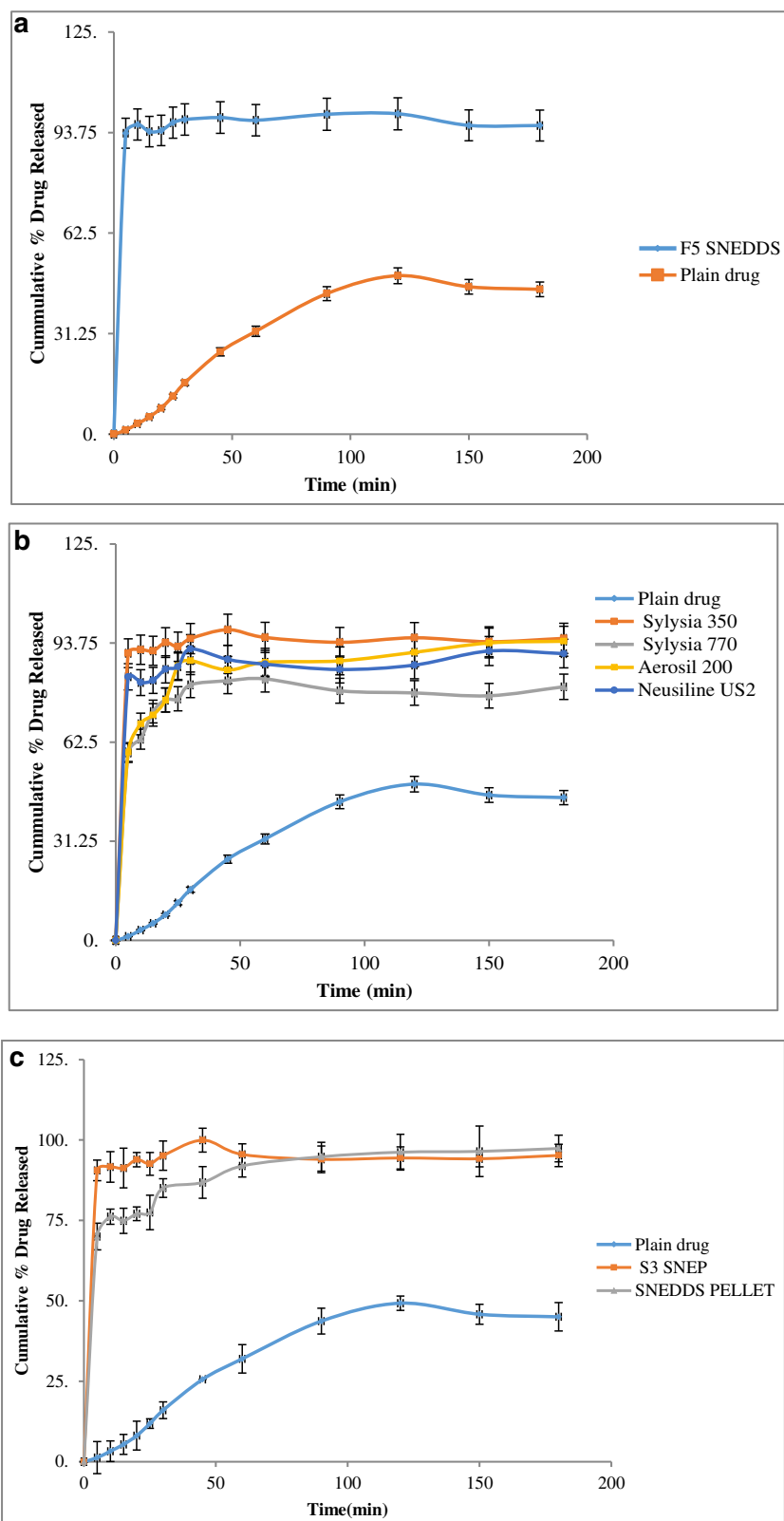
Fig. 4. **a** *In vitro* dissolution profiles in phosphate buffer (pH 7.4; mean ± SD; $n = 3$) of F5 L-SNEDDS and plain drug. **b** *In vitro* dissolution profiles in phosphate buffer (pH 7.4; mean ± SD; $n = 3$) of F5 L-SNEDDS with adsorbents of Sylysia 350, Sylysia 770, Aerosil 200, Neusilin US2, and plain drug. **c** *In vitro* dissolution profiles in phosphate buffer (pH 7.4; mean ± SD; $n = 3$) of S3 SNEP, pellet, and plain drug
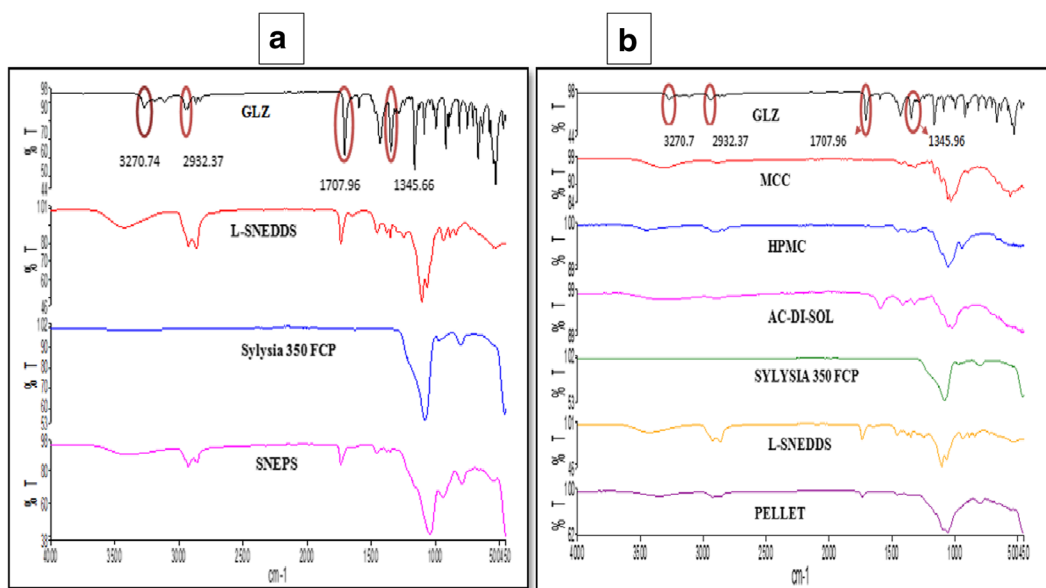
Fig. 5. **a** FTIR overlay of drug, L-SNEDDS, Sylysia 350, and S3 SNEP. **b** FTIR overlay of the drug, MCC, HPMC, Ac-di-sol, Sylysia 350, L-SNEDDS, and pellet
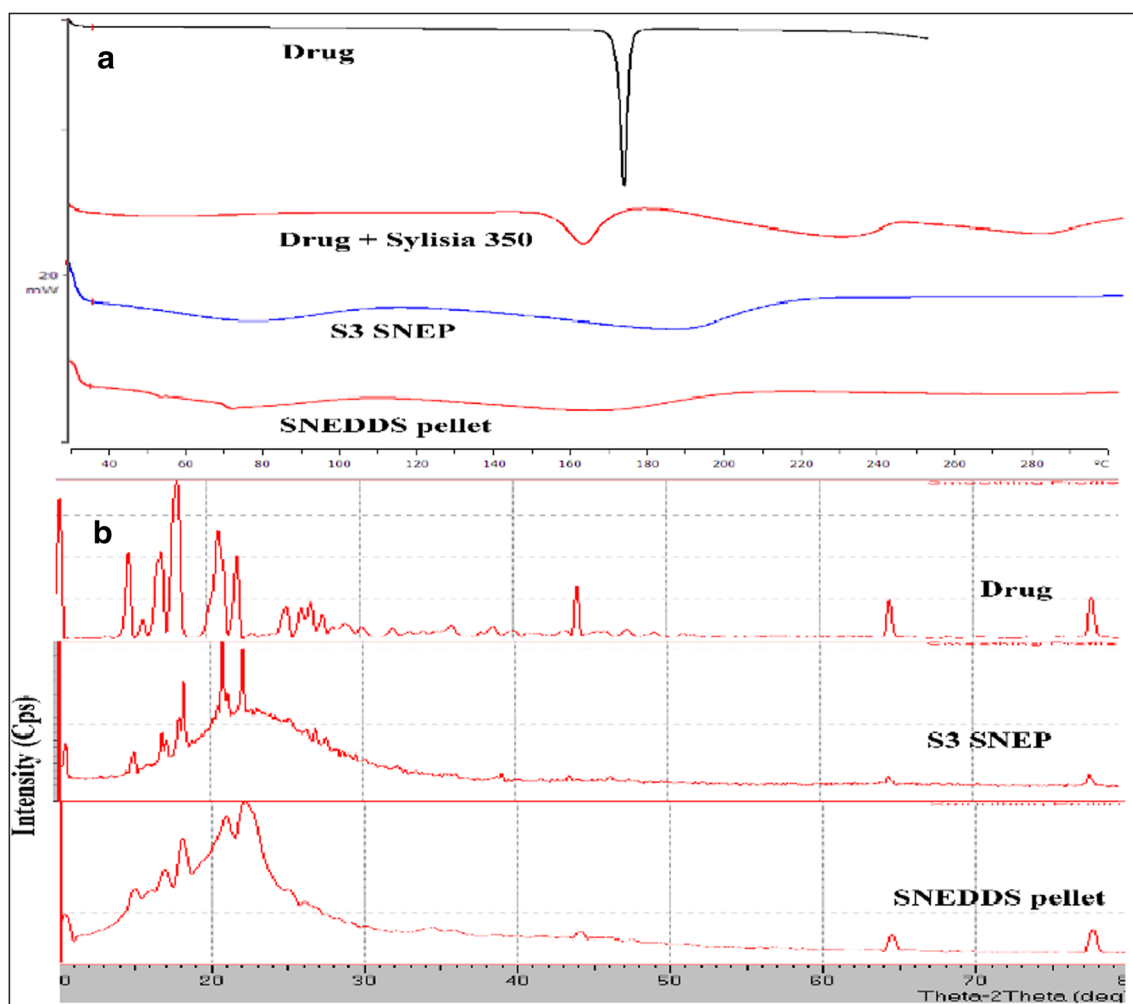

Fig. 6. **a** Overlay of differential scanning calorimetric thermograms of drug, drug + Sylysia 350 FCP, optimized S3 SNEP, and SNEDDS pellet. **b** Overlay of X-ray diffractograms of drug, S3 SNEP, and SNEDDS pellet
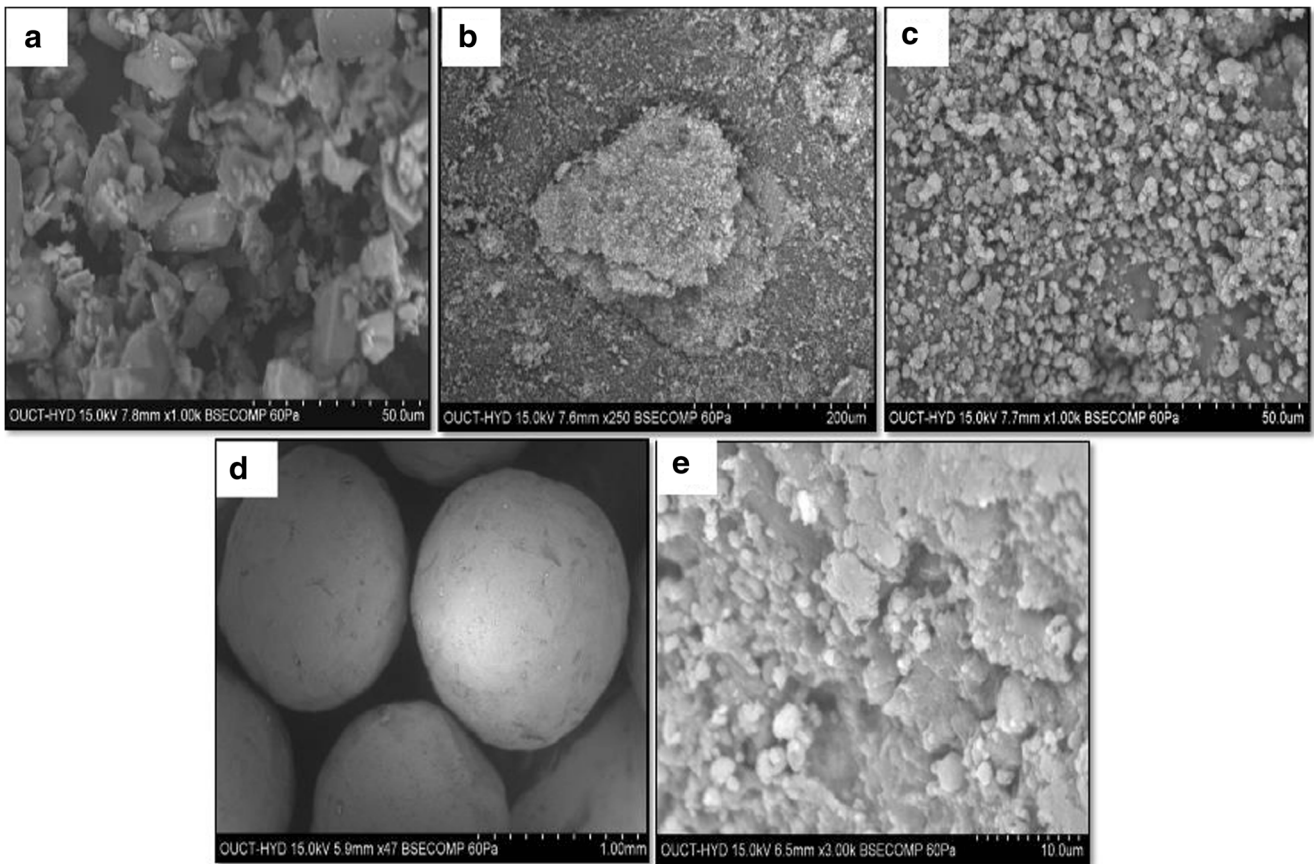
Fig. 7. Scanning electron microscopy images of **a** drug, **b** Sylysia 350, **c** S3 SNEP, **d** S-SNEDDS at 1-mm scale, and **e** S-SNEDDS at 10-μm scale

Pharmacokinetics

The plasma drug concentration *versus* time profile of plain drug suspension, L-SNEDDS, SNEP, and pellets subsequent to oral administration is depicted in Fig. 8,

and pharmacokinetic parameters are given in Table III. Unlike the plain drug, L-SNEDDS exhibited significantly higher plasma drug profiles followed by pellets and SNEP. The C_{max} values of L-SNEDDS (3639.7 ± 120 ng/mL), SNEP (2106.08 ± 115 ng/mL), and pellets ($2585.73 \pm$
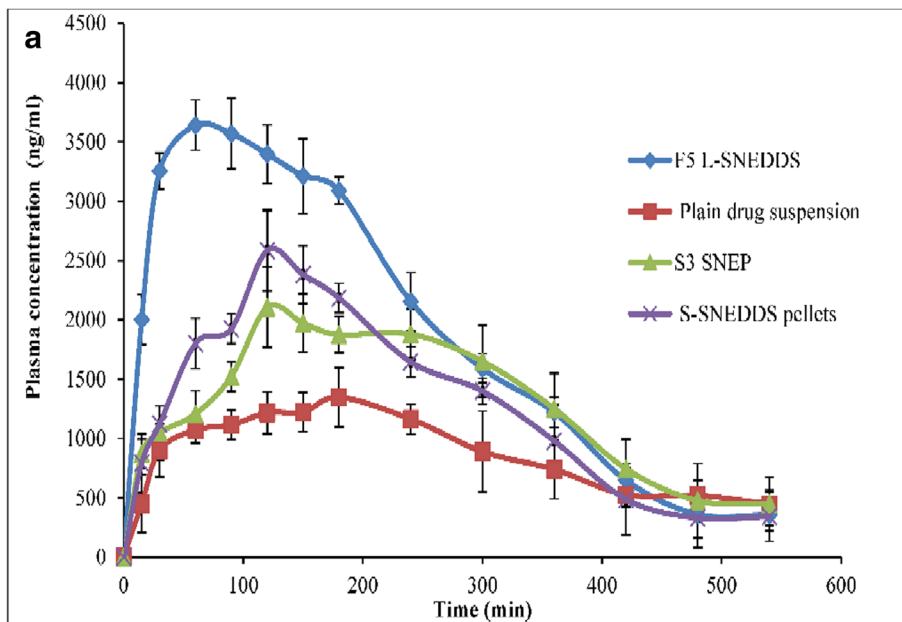

Fig. 8. Pharmacokinetic profiles in male Wistar rats ($n = 6$) of drug in plasma following oral administration of plain drug suspension, L-SNEDDS, SNEP (S3), and SNEDDS pellets

Table III. Pharmacokinetic parameters of drug (6 mg/kg) in Wistar rats following oral administration of plain drug, L-SNEDDS, S3-SNEP, and pellets (mean ± SD; $n = 6$)

PK parameter (units)	Plain drug suspension	L-SNEDDS (F5)	SNEP (S3)	Pellets
$AUC_{(0-t)}$ (ng * h/mL)	8264.46 ± 102	17,445.78 ± 125	12,095.86 ± 132	11,962.44 ± 122
$AUC_{(0-\alpha)}$ (ng * h/mL)	11,463.85 ± 105	18,471.90 ± 128	22,539.19 ± 135	13,114.83 ± 125
C_{max} (ng/mL)	1347.81 ± 118	3639.73 ± 120	2106.08 ± 115	2585.73 ± 130
T_{max} (h)	3.00	1.00	2.00	2.00
K_{el} (1/h)	0.13 ± 0.04	0.33 ± 0.06	0.04 ± 0.01	0.30 ± 0.07
$t_{1/2}$ (h)	5.48 ± 1.2	2.07 ± 0.15	16.53 ± 2.5	2.33 ± 0.5
V_{z-obs} (L/kg)	4.14 ± 1.2	0.97 ± 0.3	6.35 ± 1.8	1.54 ± 0.6
CL_{z-obs} (L/h/kg)	0.52 ± 0.2	0.32 ± 0.12	0.27 ± 0.1	0.46 ± 0.13
MRT (h)	8.03 ± 0.8	3.74 ± 0.6	17.87 ± 1.5	4.48 ± 0.5
% relative bio-availability (F_{rel})[a]	100.00	211.09	146.36	144.75

[a] F_{rel} calculated for the average AUC values

130 ng/ml) were approximately twofolds higher than plain drug suspension (1347.81 ± 118 ng/mL). However, T_{max} in case of L-SNEDDS and SNEP was 1–2 h compared to 3 h for the plain drug. Area under the curve (AUC_{0-t}), which indicates the extent of absorption, was higher around twofolds for L-SNEDDS compared to suspension. In total, it is clear that the degree of absorption of GCZ had been evidently enhanced from the prepared formulations, which was due to existence of hydrophobic drug in tiny emulsion globules that makes the availability of drug in a dissolved state across gastrointestinal (GI) membrane and thereby lymphatic transportation during intestinal trans-cellular corridor (51). Another reason for high bioavailability of GCZ in SNEDDS is attributed to its ability to get dispersed in GI fluid, crossing the intestinal epithelial layers, possibility of lymphatic uptake, bypassing the p-glycoprotein efflux system, and cytochrome P-450 mediated drug metabolism (52). The present study outcomes too favored absorption of GCZ from the preparations due to the medium chain triglycerides of Capmul MCM C8 NF, which improves lymphatic absorption (49,50). Studies also suggest that the lipid-based drug delivery systems consisting of lengthy chain and intermediate fatty acids deliver the drugs to gastric lymph and evade the portal movement (41).

Anti-Diabetic Activity

The mean percentage reduction in blood glucose level in Wistar rats after administration of plain GCZ, L-SNEDDS, SNEP, and pellet is shown in Table IV. The results demonstrated a considerable improvement in biological behavior of L-SNEDDS, SNEP, and pellet than plain GCZ, and there was no remarkable variation among the L-SNEDDS, SNEP, and pellet. The reduction in the glucose levels could be due to effective solubilization of GCZ in SNEDDS leading to faster and complete absorption (37).

CONCLUSION

Self-nanoemulsifying system for GCZ was formulated and optimized using Capmul MCM C8 NF (30%), Cremophor RH 40 (20%), and Transcutol-HP (50%) as oil, surfactant, and co-surfactant, respectively. D-optimal design was applied to study the effects of variables on responses, and further, an optimum formulation was selected by numerical and graphical optimization. The final composition yielded a translucent nanoemulsion with a mean particle size < 200 nm on dilution. To increase the ease of handling, L-SNEDDS has been successfully transformed into SNEP and pellet. *In vitro* dissolution studies revealed the ability of lipid carriers to

Table IV. Anti-diabetic activity of GCZ formulations in normoglycemic Wistar rats after oral administration (25 mg/kg, $n = 6$)

Time (h)	Blood glucose level (mg/dl)				
	Control	Plain drug suspension	L-SNEDDS	SNEP	Pellets
0	79.65 ± 2.27	83.20 ± 3.61	74.63 ± 1.54	76.31 ± 3.42	82.88 ± 3.29
0.5	155.23 ± 1.26	136.22 ± 6.84	104.43 ± 1.61	106.29 ± 4.03	112.63 ± 4.38
1	136.88 ± 2.79	118.37 ± 2.88	92.91 ± 1.21	94.02 ± 3.70	104.55 ± 2.58
2	106.66 ± 0.56	102.12 ± 2.63	86.79 ± 3.56	88.71 ± 3.58	96.45 ± 1.77
4	100.48 ± 4.30	93.50 ± 3.69	73.57 ± 1.25	72.68 ± 5.40	79.11 ± 1.76
6	94.30 ± 1.16	83.93 ± 0.91	76.23 ± 1.33	74.61 ± 2.70	81.32 ± 4.18
12	96.36 ± 3.46	82.78 ± 5.01	73.81 ± 2.37	79.66 ± 3.54	87.49 ± 3.61
24	99.52 ± 2.60	82.77 ± 4.82	74.45 ± 3.64	75.14 ± 3.44	79.91 ± 1.35

enhance the drug dissolution in a significant manner, while plain form failed in similar prospect. Similarly, *in vivo* plasma concentration profiles of SNEDDS were superior with higher C_{max} and AUC values compared to plain drug suspension as a result of higher diffusion and dissolution achieved by smaller droplet size of nanoemulsion. Correspondingly, SNEDDS formulation had shown a significant decrease in blood glucose levels in normoglycemic glucose tolerance tests. To conclude, the use of SNEDDS for delivering GCZ could be a potential approach for combating the current therapy.

ACKNOWLEDGMENTS

COMPLIANCE WITH ETHICAL STANDARDS

Conflict of Interest The authors declare that there are no conflicts of interest.

Publisher's Note Springer Nature remains neutral with regard to jurisdictional claims in published maps and institutional affiliations.

REFERENCES

1. Aggarwal BB, Shishodia S, Sandur SK, Pandey MK, Sethi G. Inflammation and cancer: how hot is the link? Biochem Pharmacol. 2006;72(11):1605–21.
2. Palmer KJ, Brogden RN. Gliclazide. Drugs. 1993;46(1):92–125.
3. Amidon GL, Lennernäs H, Shah VP, Crison JR. A theoretical basis for a biopharmaceutic drug classification: the correlation of in vitro drug product dissolution and in vivo bioavailability. Pharm Res. 1995;12(3):413–20.
4. Desai KGH, Kulkarni AR, Aminabhavi TM. Solubility of rofecoxib in the presence of methanol, ethanol, and sodium lauryl sulfate at (298.15, 303.15, and 308.15) K. J Chem Eng Data. 2003;48(4):942–5.
5. Delrat P, Paraire M, Jochemsen R. Complete bioavailability and lack of food-effect on pharmacokinetics of gliclazide 30 mg modified release in healthy volunteers. Biopharm Drug Dispos. 2002;23(4):151–7.
6. Bandarkar FS, Khattab IS. Lyophilized gliclazide poloxamer, solid dispersions for enhancement of in vitro dissolution and in vivo bioavailability. Int J Pharm Pharm Sci. 2011;3(2):122–7.
7. Moyano J, Arias-Blanco M, Gines J, Giordano F. Solid-state characterization and dissolution characteristics of gliclazide-β-cyclodextrin inclusion complexes. Int J Pharm. 1997;148(2):211–7.
8. Averineni RK, Shavi GV, Ranjan OP, Deshpande PB, Kumar GA, Nayak UY, et al. Formulation of gliclazide encapsulated chitosan nanoparticles: in vitro and in vivo evaluation. Nano-Formulation. 2012;77–85.
9. Devarajan PV, Sonavane GS. Preparation and in vitro/in vivo evaluation of gliclazide loaded eudragit nanoparticles asa sustained release carriers. Drug Dev Ind Pharm. 2007;33:101–11.
10. Naik JBMV, Shevalkar GB, Patil KV, Patil JS, Yadava S, Verma U. Formulation and evaluation of poly (L-lactide-co-caprolactone) loaded gliclazide biodegaradable nanoparticles as a control release carrier. Int J Drug Deliv. 2013;5:300–8.
11. Seo YG, Kim DH, Ramasamy T, Kim JH, Marasini N, Oh YK, et al. Development of docetaxel-loaded solid self-nanoemulsifying drug delivery system (SNEDDS) for enhanced chemotherapeutic effect. Int J Pharm. 2013;452(1):412–20.
12. Date AA, Desai N, Dixit R, Nagarsenker M. Self-nanoemulsifying drug delivery systems: formulation insights, applications and advances. Nanomedicine. 2010;5(10):1595–616.
13. Basalious EB, Shawky N, Badr-Eldin SM. SNEDDS containing bioenhancers for improvement of dissolution and oral absorption of lacidipine. I: development and optimization. Int J Pharm. 2010;391(1):203–11.
14. Inugala S, Eedara BB, Sunkavalli S, Dhurke R, Kandadi P, Jukanti R, et al. Solid self-nanoemulsifying drug delivery system (S-SNEDDS) of darunavir for improved dissolution and oral bioavailability: in vitro and in vivo evaluation. Eur J Pharm Sci. 2015;74:1–10.
15. Woo JS, Song YK, Hong JY, Lim SJ, Kim CK. Reduced food-effect and enhanced bioavailability of a self-microemulsifying formulation of itraconazole in healthy volunteers. Eur J Pharm Sci. 2008;33(2):159–65.
16. Sharma D, Maheshwari D, Philip G, Rana R, Bhatia S, Singh M, et al. Formulation and optimization of polymeric nanoparticles for intranasal delivery of lorazepam using Box-Behnken design: in vitro and in vivo evaluation. Biomed Res Int. 2014;2014:1–14.
17. Wankhade VP, Atram SC, Bobade NN, Pande SD, Tapar KK. Formulation and optimization of SNEDDS of gliclazide using response surface methodology. Asian J Pharm 2014;6(4).
18. Patel J, Patel A, Raval M, Sheth N. Formulation and development of a self-nanoemulsifying drug delivery system of irbesartan. J Adv Pharm Technol Res. 2011;2(1):9–16.
19. Khan AW, Kotta S, Ansari SH, Sharma RK, Ali J. Self-nanoemulsifying drug delivery system (SNEDDS) of the poorly water-soluble grapefruit flavonoid naringenin: design, characterization, in vitro and in vivo evaluation. Drug Deliv. 2015;22(4):552–61.
20. Dash RN, Mohammed H, Humaira T, Reddy AV. Solid supersaturatable self-nanoemulsifying drug delivery systems for improved dissolution, absorption and pharmacodynamic effects of glipizide. J Drug Deliv Sci Technol. 2015;28:28–36.
21. MaraMainardes LGM. Application of a validated HPLC-PDA method for the determination of melatonin content and its release from poly (lactic acid) nanoparticles. J Pharmaceut Anal. 2017;7(6):388–93.
22. Craig D, Lievens H, Pitt K, Storey D. An investigation into the physico-chemical properties of self-emulsifying systems using low frequency dielectric spectroscopy, surface tension measurements and particle size analysis. Int J Pharm. 1993;96(1–3):147–55.
23. Nazzal S, Khan MA. Response surface methodology for the optimization of ubiquinone self-nanoemulsified drug delivery system. AAPS PharmSciTech. 2002;3(1):23–31.
24. Pund S, Shete Y, Jagadale S. Multivariate analysis of physico-chemical characteristics of lipid based nanoemulsifying cilostazol—quality by design. Colloids Surf B Biointerfaces. 2014;115:29–36.
25. Rahman MA, Iqbal Z, Hussain A. Formulation optimization and in vitro characterization of sertraline loaded self-nanoemulsifying drug delivery system (SNEDDS) for oral administration. J Pharm Investig. 2012;42(4):191–202.
26. Kallakunta VR, Bandari S, Jukanti R, Veerareddy PR. Oral self-emulsifying powder of lercanidipine hydrochloride: formulation and evaluation. Powder Technol. 2012;221:375–82.
27. Tarr BD, Yalkowsky SH. Enhanced intestinal absorption of cyclosporine in rats through the reduction of emulsion droplet size. Pharm Res. 1989;6(1):40–3.
28. Date AA, Nagarsenker M. Design and evaluation of self-nanoemulsifying drug delivery systems (SNEDDS) for cefpodoxime proxetil. Int J Pharm. 2007;329(1):166–72.
29. Gera S, Talluri S, Rangaraj N, Sampathi S. Formulation and evaluation of naringenin nanosuspensions for bioavailability enhancement. AAPS PharmSciTech. 2017;18(8):3151–62.
30. Neerati P, Bedada SK. Effect of diosmin on the intestinal absorption and pharmacokinetics of fexofenadine in rats. Pharmacol Rep. 2015;67(2):339–44.
31. Chavda H, Patel J, Chavada G, Dave S, Patel A, Patel C Self-nanoemulsifying powder of isotretinoin:preparation and characterization. J Powder Technol. 2013;2013.

32. Sunkavalli S, Eedara BB, Janga KY, Velpula A, Jukanti R, Bandari S. Preparation and characterization of docetaxel self-nanoemulsifying powders (SNEPs): a strategy for improved oral delivery. Korean J Chem Eng. 2015.

33. Abbaspour M, Jalayer N, Sharif Makhmalzadeh B. Development and evaluation of a solid self-nanoemulsifying drug delivery system for loratadin by extrusion-spheronization. Adv Pharm Bull. 2014;4(2):113–9.

34. Miao Y, Chen G, Ren L, Pingkai O. Characterization and evaluation of selfnanoemulsifying sustained-release pellet formulation of ziprasidone with enhancedbioavailability and no food effect. Drug Deliv. 2016;23(7):2163–72.

35. Elkordy AA, Essa EA, Dhuppad S, Jammigumpula P. Liquisolid technique to enhance and to sustain griseofulvin dissolution: effect of choice of non-volatile liquid vehicles. Int J Pharm. 2012;434(1):122–32.

36. Srikanth CH, Chaira T, Sampathi S, Sreekumar V, Bambal RB. Correlation of in vitro and in vivo plasma protein binding using ultracentrifugation and UPLC-tandem mass spectrometry. Analyst. 2013;138(20):6106–16.

37. Zawar LR, Bari SB. Preparation, characterization and in vivo evaluation of antihyperglycemic activity of microwave generated repaglinide solid dispersion. Chem Pharm Bull. 2012;60(4):482–7.

38. Sunkavalli S, Eedara BB, Janga KY, Velpula A, Jukanti R, Bandari S. Preparation and characterization of docetaxel self-nanoemulsifying powders (SNEPs): a strategy for improved oral delivery. Korean J Chem Eng. 2016;33(3):1115–24.

39. Taha EI, Al-Saidan S, Samy AM, Khan MA. Preparation and in vitro characterization of self-nanoemulsified drug delivery system (SNEDDS) of all-trans-retinol acetate. Int J Pharm. 2004;285(1):109–19.

40. Constantinides PP, Scalart J-P, Lancaster C, Marcello J, Marks G, Ellens H, et al. Formulation and intestinal absorption enhancement evaluation of water-in-oil microemulsions incorporating medium-chain glycerides. Pharm Res. 1994;11(10):1385–90.

41. Porter CJ, Trevaskis NL, Charman WN. Lipids and lipid-based formulations: optimizing the oral delivery of lipophilic drugs. Nat Rev Drug Discov. 2007;6(3):231–48.

42. Nielsen FS, Petersen KB, Müllertz A. Bioavailability of probucol from lipid and surfactant based formulations in minipigs: influence of droplet size and dietary state. Eur J Pharm Biopharm. 2008;69(2):553–62.

43. Gupta S, Chavhan S, Sawant KK. Self-nanoemulsifying drug delivery system for adefovir dipivoxil: design, characterization, in vitro and ex vivo evaluation. Colloids Surf A Physicochem Eng Asp. 2011;392(1):145–55.

44. Zhao Y, Wang C, Chow AH, Ren K, Gong T, Zhang Z, et al. Self-nanoemulsifying drug delivery system (SNEDDS) for oral delivery of zedoary essential oil: formulation and bioavailability studies. Int J Pharm. 2010;383(1):170–7.

45. Takeuchi H, Nagira S, Yamamoto H, Kawashima Y. Solid dispersion particles of amorphous indomethacin with fine porous silica particles by using spray-drying method. Int J Pharm. 2005;293(1):155–64.

46. Balakrishnan P, Lee B-J, Oh DH, Kim JO, Hong MJ, Jee J-P, et al. Enhanced oral bioavailability of dexibuprofen by a novel solid self-emulsifying drug delivery system (SEDDS). Eur J Pharm Biopharm. 2009;72(3):539–45.

47. Newton M, Petersson J, Podczeck F, Clarke A, Booth S. The influence of formulation variables on the properties of pellets containing a self-emulsifying mixture. J Pharm Sci. 2001;90(8):987–95.

48. Bari A, Chella N, Sanka K, Shastri NR, Diwan PV. Improved anti-diabetic activity of glibenclamide using oral self-nanoemulsifying powder. J Microencapsul. 2015;32(1):54–60.

49. Mohd AB, Sanka K, Bandi S, Diwan PV, Shastri N. Solid self-nanoemulsifying drug delivery system (S-SNEDDS) for oral delivery of glimepiride: development and antidiabetic activity in albino rabbits. Drug Deliv. 2015;22(4):499–508.

50. Janga KY, Jukanti R, Sunkavalli S, Velpula A, Bandari S, Kandadi P, et al. In situ absorption and relative bioavailability studies of zaleplon loaded self-nanoemulsifying powders. J Microencapsul. 2013;30(2):161–72.

51. Gershanik T, Benita S. Self-dispersing lipid formulations for improving oral absorption of lipophilic drugs. Eur J Pharm Biopharm. 2000;50(1):179–88.

52. Rao SVR, Shao J. Self-nanoemulsifying drug delivery systems (SNEDDS) for oral delivery of protein drugs: I. Formulation development. Int J Pharm. 2008;362(1):2–9.